CO_2 hydrogenation to liquid hydrocarbons via modified Fischer–Tropsch over alumina-supported cobalt catalysts: Effect of operating temperature, pressure and potassium loading

Phathutshedzo R Khangale [1 *], Reinout Meijboom [2], Kalala Jalama [1]

[1] Department of Chemical Engineering, Faculty of Engineering and the Built Environment, University of Johannesburg, Doornfontein 2028, Johannesburg, South Africa.

[2] Department of Chemical Sciences, Faculty of Science, University of Johannesburg, Auckland Park 2006, Johannesburg, South Africa.

** Corresponding Author. E-mail: pkhangale@uj.ac.za (P.R. Khangale), Tel: +27-11-5596314, Fax: +27-11-5596159*

Abstract

The effect of promoting 15%Co/Al_2O_3 catalyst with potassium on CO_2 hydrogenation to longer-chain hydrocarbons was investigated. The catalysts used in this study were synthesized using an incipient wetness impregnation of the support with nitrate solutions. All catalysts were supported on γ-alumina and promoted with potassium (0 – 8%). The synthesized catalysts were characterized by XRD, BET, XPS, TPR and CO_2-TPD analyses. The catalysts were evaluated for CO_2 hydrogenation using a fixed-bed tube reactor. The CO_2 conversion was found to increase with both the reaction temperature and pressure. The TPR data revealed that potassium limited the reduction of the catalyst, decreased the selectivity to methane and increased the selectivity to C_{2+} hydrocarbons. The maximum C_{2+} yield of 10.2%, with CO_2 conversion of 42.3%, was obtained when 6 wt.% of potassium was added to the catalyst. It is believed that during the CO_2 hydrogenation process over the catalysts that were promoted with potassium, CO_2 is first converted to CO via reverse–water–gas–shift reaction, followed by subsequent hydrogenation of CO to hydrocarbons.

Keywords:

Co/Al_2O_3 catalyst; CO_2 hydrogenation; potassium; pressure; temperature.

1. Introduction

The reduction of CO_2 released into the atmosphere has become a central research focus nowadays since carbon dioxide is one of the main contributors to the green-house effect; its global production is on the rise, leading to the global temperature increases and climate change due to the "greenhouse effect" [1 – 2]. The first approach to address CO_2 emissions, which has been intensely probed in the most recent years and which has been recently applied for the first time to a large-scale power station in Canada [3], is Carbon Capture and Storage (CCS) [4]. This involves permanent CO_2 storage deep underground in explicit geological locations. Carbon Capture and Utilization (CCU) processes are alternatives to this technology and which involve the chemical transformation of CO_2 to valuable carbon-bearing products. Among them, the transformation of CO_2 into gasoline is of extreme importance because the extensive market of these products would potentially reduce the global CO_2 productions, at the same time minimizing the consumption of fossil fuels. Usually, carbon dioxide could be hydrogenated to liquid fuels, both by direct and indirect methods. In the indirect method, CO_2 is converted to methanol, which can be then be converted into hydrocarbons through the commercially existing methanol-to-gasoline (MTG) method [5]. On the other hand, the direct method involves the conversion of CO_2 to CO via the reverse–water–gas–shift (RWGS) reaction followed by hydrogenation of CO to hydrocarbons through the Fischer-Tropsch (FT) process, ultimately accompanied by a product upgrading step [2, 6 – 7]. Still, as compared with the indirect method, the direct method would be more cost-effective and energy-efficient. Thermodynamically, the conversion of CO_2 by reverse water-gas-shift at low temperature is limited to some degree. As a result, many researchers studied the CO_2 hydrogenation to hydrocarbons at high temperatures (300 – 400 °C) [8 – 9]. To date, between the two commercially used FT catalysts (Fe and Co), Fe is often chosen for FT initiated from CO_2 since Co has been reported to act as a methanation catalyst at higher temperatures [10 – 12]. In contrast, very few research reports have been published on CO_2 hydrogenation to hydrocarbons using cobalt-based catalysts. In traditional FT reactions conducted at low temperatures (< 250 °C), cobalt-based catalysts are commonly used because of their high catalytic activity, high yields of heavyweight hydrocarbons and high stability relative to their counter iron-based catalysts and lower price compared to noble metals such as ruthenium-based catalysts [13]. The literature reveals that cobalt-based catalysts show a good catalytic activity during CO_2 hydrogenation to fuel [14 – 16]. In addition, supplementary metals such as Pt, Ru, Cu and Pd are also added to improve the formation of CO, because cobalt is not active for WGS and RWGS reactions. During CO_2 hydrogenation, the extent of hydrogenation of surface-adsorbed intermediates is greater because of the slower rate of adsorption of CO_2 as compared to CO hydrogenation, promoting the formation of

methane, at the same time limiting chain growth [17]. Subsequently, there is still a significant challenge related to increasing reactivity for chain growth and defeating the formation of methane. According to Akin *et al* [17], methane is the most dominating product during CO_2 hydrogenation using Co/Al_2O_3 catalyst. Promoters such as Na [9] and K [18] have been widely investigated for Fe-based CO_2 hydrogenation. These promoters are reported to inhibit methane generation and promote chain growth probability and boost alkene production. Moreover, the promoter's influence on the selectivity of the product has been reported to be dependent on its concentration.

Fundamental differences in the mechanism of CO hydrogenation (during normal FT reaction) and CO_2 hydrogenation (in modified FT reaction) are still not well-understood. This has made it difficult to design catalysts that can efficiently convert CO_2 into liquid fuels. The limited data reported in the literature [19 – 23] suggest that the promotion of cobalt-based catalysts with alkali metals offers the potential for improving the selectivity of CO_2 hydrogenation toward long-chain hydrocarbons. However, no systematic study has been conducted to determine the optimum loading of promoters and the operating conditions most favorable to the process. Furthermore, it is not clearly understood whether the promoting effect of alkali metals is due to geometric or electronic effects. This study aims to investigate the effect of operating temperature, pressure, and potassium promoter on CO_2 hydrogenation to longer chain hydrocarbons over $15\%Co/Al_2O_3$ Fischer–Tropsch catalysts.

2. Experimental details

2.1 . Catalyst preparation and characterization

The catalysts were prepared by incipient wetness impregnation of the alumina support (from Sigma-Aldrich) using an aqueous solution of cobalt nitrate (to achieve 15 wt.% Co in the catalyst) and dried in air at 120 °C overnight. The samples were then calcined in air at 500 °C for 10 hours. The catalysts promoted with potassium underwent an additional step of incipient wetness impregnation using a potassium nitrate solution. The catalysts were prepared to give the weight percentage of potassium to be 0–8 wt.%. The promoted catalysts were also dried in air overnight at 120 °C and then calcined in air at 500 °C for 10 hours.

The surface area and pore distribution for the synthesized catalysts were determined using Brunauer-Emmett-Teller (BET) analyses that were performed on a Micromeritics Tristar 3000 using N_2. X-ray diffraction (XRD) analyses were used to determine the cobalt phase in the catalysts before, after reduction, and after the FT reaction following the procedure described in an earlier study [24]. CO_2–Temperature programmed desorption (CO_2–TPD) measurements were conducted to investigate

the basicity of the catalysts on the same apparatus that was used for temperature-programmed reduction (TPR) analyses, described later in this section. X–ray photoelectron spectroscopy (XPS) measurements were conducted on a SPECS PHOIBOS 150 hemispherical analyzer to obtain information on the catalyst surface composition. XPS data were corrected by setting the oxidic O1s binding energy to 531.5 eV. TPR analyses were performed using an apparatus constructed at the University to compare the catalysts' behavior during the reduction in the presence of 5% H_2/Ar. The calcined catalyst samples (100 mg) were initially loaded in a stainless steel tube reactor (ID: 9 mm) and degassed using helium gas (30 ml/min) at 300 °C for 1 hour and cooled to room temperature. The samples were subsequently subjected to a continuous flow of the reducing gas mixture (30 ml/min) while the temperature was increased to 700 °C (10 ^oC/min). The flow-rate of the reducing gas was kept at 30 ml/min for all the analyses and a thermal conductivity detector (TCD) was located at the reactor outlet to detect changes in H_2 concentration.

All reduced catalysts used in this study were prepared by reducing fresh calcined catalyst samples in the same tube reactor used to test catalysts for CO_2 hydrogenation, as described in the next section. Both reduced and spent catalysts were passivated with 5%O_2/He before being removed from the reactor to avoid oxidation.

2.2 Catalyst testing

The catalysts were evaluated for carbon dioxide hydrogenation using a stainless-steel fixed-bed tubular reactor with the internal diameter of 16mm and length of 220 mm constructed at the university. About 0.5g of the catalyst was loaded in the reactor and various parameters such as the operating temperature, pressure and potassium loading were evaluated. The catalysts were activated by reducing with pure H_2 for 17 hours to convert cobalt oxide to metallic cobalt. The flow rate of the reducing gas mixture was set to 30 ml/min at atmospheric pressure. The temperature was elevated from room temperature to 350 ^oC at a rate of 10 ^oC per minute and kept there for 17 hours.

CO_2 hydrogenation runs were performed using a feed containing 10% N_2, 22.5% CO_2 and 67.5% H_2. The outlet gas products were analyzed using a Dani master GC equipped with TCD connected to a carboxen 1000 column and an FID connected to a fused silica capillary column 30 m long with 0.32 mm diameter.

The hydrocarbon distribution was calculated based on the total carbon moles with the unit of C-mole% on all evaluated catalysts and the equations used are listed below.

N_2 was used in the reaction feed gas to serve as an internal standard that allowed us to take gas expansion into account for accurate calculations of the CO_2 conversion.

The $\%CO_2$ conversion was calculated as follows:

$$\%CO_2 \text{ conversion} = \frac{\%CO_{2in} - \left(\frac{\%N_{2in}}{\%N_{2out}}\right) \times \%CO_{2out}}{\%CO_{2in}} \times 100\% \quad \text{.....(1)}$$

The rate of CO_2 conversion was calculated as:

$$-rCO_2 = \dot{n}_{T_{in}} \times \%CO_{2in} \times \frac{\%CO_2 \text{ Conversion}}{100} \quad \text{.....(2)}$$

The rate of CH_4 production was calculated as:

$$rCH_4 = \dot{n}_{T_{out}} \times \frac{\%CH_{4out}}{100} \quad \text{.....(3)}$$

The selectivity of CH_4 was expressed as follows:

$$CH_4 \text{ selectivity} = \frac{rCH_4}{-rCO_2} \times 100\% \quad \text{.....(4)}$$

The selectivity of C_2-C_4 was calculated using the following expression

$$C_n \text{selectivity} = \frac{[(rC_nH_{n+1} + rC_nH_{n+2}) \times n]}{-rCO_2} \times 100\% \quad \text{.....(5)}$$

Where n is the number of carbons

The rate of CO production was calculated as:

$$rCO = \dot{n}_{T_{out}} \times \frac{\%CO_{out}}{100} \quad \text{.....(6)}$$

The selectivity of CO was expressed as follows:

$$CO \text{ selectivity} = \frac{rCO}{-rCO_2} \times 100\% \quad \text{.....(7)}$$

The selectivity of C_{5+} was calculated as follows:

$$C_{5+}\text{selectivity} = 100\% - CH_4\text{selectivity} - \sum(C_2 + C_3 + C_4)\ \text{selectivity} - CO\ selectivity$$

……....(8)

The C_{2+} selectivity was calculated as follows:

$$C_{2+}\text{selectivity} = \sum(C_2 + C_3 + C_4)\ \text{selectivity} + C_{5+}\text{selectivity}$$ ……..….(9)

The C_{2+} yield was calculated as follows:

$$C_{2+}\text{yield} = \frac{CO_{2conversion} \times C_{2+}selectivity}{100\%}$$ ……..(10)

The CH_4 yield was calculated as:

$$CH_4\text{yield} = \frac{CO_{2conversion} \times CH_4selectivity}{100\%}$$ ……..……..(11)

3. Results and Discussion

3.1. Catalyst characterization

3.1.1. Brunauer-Emmett and Teller (BET) analysis

The BET analyses were performed on both potassium–promoted and unpromoted calcined fresh catalysts. The BET surface area, total pore volume, and average pore sizes for 15%Co/Al_2O_3 catalysts with different potassium loadings are reported in Table 1.

Table 1: Summary of BET results

Catalyst	**BET surface area [m^2/g]**	**Pore volume [cm^3/g]**	**Pore size [nm]**
15%Co/Al_2O_3	124	0.193	6.20
15%Co-1%K/Al_2O_3	107	0.176	6.56
15%Co-3%K/Al_2O_3	105	0.174	6.61
15%Co-5%K/Al_2O_3	72.2	0.129	7.12
15%Co-6%K/Al_2O_3	56.2	0.101	7.17
15%Co-8%K/Al_2O_3	28.2	0.013	1.88

The BET surface area and pore volume of the calcined 15%Co/Al_2O_3 catalysts decreased with the addition of potassium. Linear regression was applied to the data (fig. 1) and the summary of ANOVA and regression statistics are reported in Tables S1 and S2 in Appendix A.

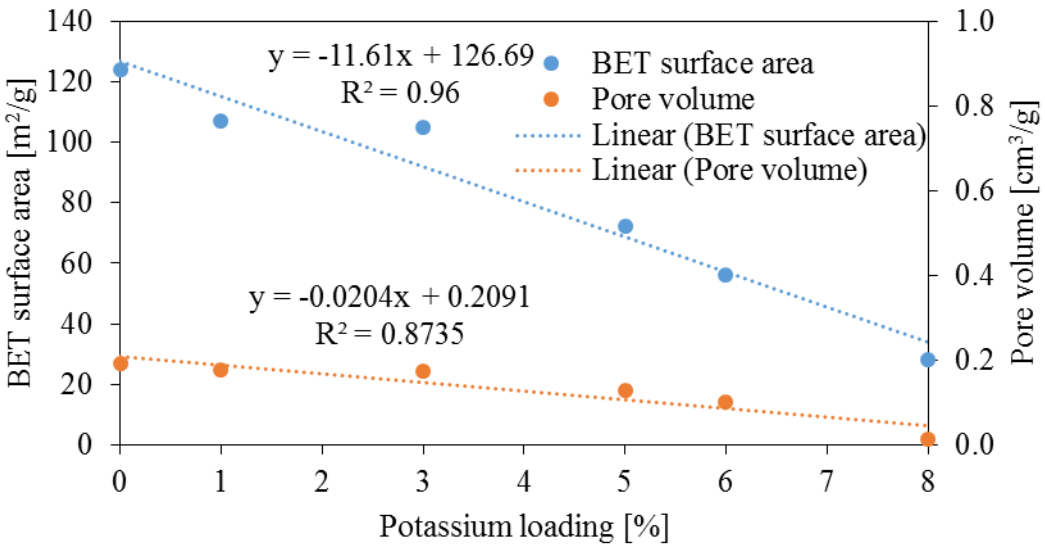

Fig. 1: BET surface area and pore volume as a function of potassium loading.

At a 95% level of confidence, the confidence interval for the slope related to the change of the BET surface area with potassium loading is (-15.06, -8.17). Since the slope of the linear trendline (-11.61) falls in this interval, there is a significant negative relationship between the BET surface area and potassium loading. Thus, 96 % (R^2 = 0.96) of the change in the BET surface area can be explained by the change in potassium loading. Similarly, the pore volume of the catalyst linearly decreases with an increasing potassium loading. However, at 8% potassium loading, a significant drop in pore volume is noticed. This was most likely the result of the partial coverage of the surface by potassium [25]. On the other hand, the average pore size was found to increase with potassium loading from 6.20 nm in the case of the unpromoted catalyst to 7.17 nm in the case of 6 wt.% potassium loading. This could indicate that some pores collapsed during the subsequent calcination step used to decompose potassium nitrate added to the catalyst. Further increase in potassium loading resulted in severe pore blockage in the catalyst as indicated by the significant and concomitant drop in BET surface area, pore-volume, and pore size.

3.1.2. X–ray diffraction analyses

XRD analyses were performed on calcined, activated, and spent catalysts. The results are presented in figure 2.

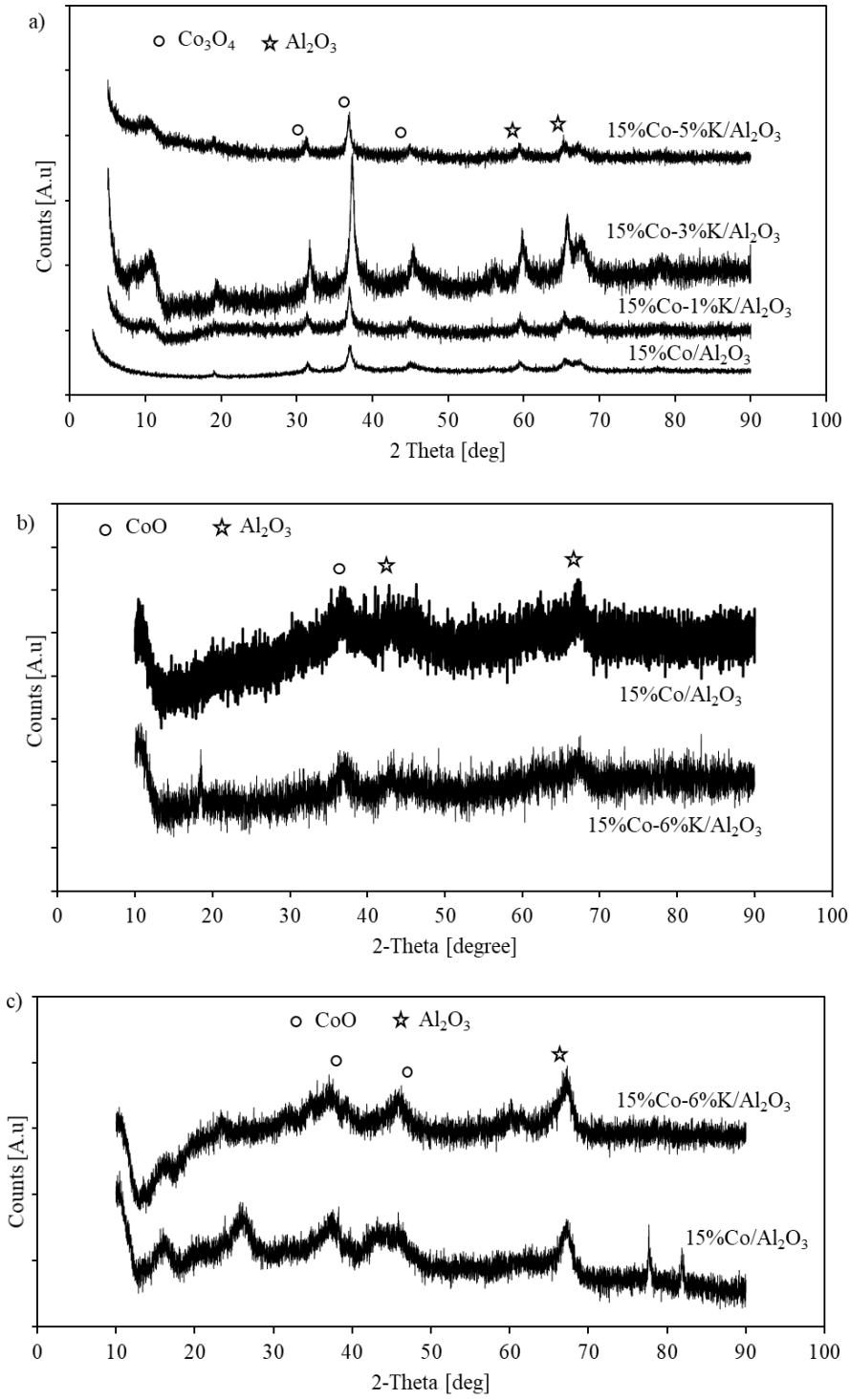

Fig. 2: XRD profiles for a) fresh-calcined, b) reduced and passivated, and c) spent catalysts.

For the calcined fresh catalyst sample (Fig. 2a), the diffraction peaks corresponding to Co_3O_4 are observed at angle 2θ of around 31°, 37° and 45°. No diffraction peaks associated with potassium were detected from the samples. This could be ascribed to the low concentration and good dispersion and the presence of amorphous phase [19]. The average particle size (Table 2) of Co_3O_4 was calculated

using the most intensive peaks associated to Co_3O_4, around 37°, using the Scherrer equation [26]. The particle size for the catalysts increased slightly with the introduction of potassium. For the unpromoted calcined catalyst, the average Co_3O_4 particle size was 9.4 nm; it increased to 13.2, 13.4 and 15.6 nm respectively after adding 1, 3 and 5% of potassium to the catalyst. For the reduced catalysts (Fig. 2b) the XRD pattern displayed three peaks at around 37°, 42° and 67° with the most intensive peak corresponding to cobalt crystallite observed at about 37.5 and 36.9° for unpromoted and 6 wt.% potassium–promoted catalysts respectively. For spent catalysts, Fig. 2c (300 °C, 5 bar, H_2/CO_2 = 3.0), the diffraction peaks were observed at 37.2° and 44.0° for the unpromoted catalyst and 36.8° and 45.6° for 6% potassium–promoted catalyst. The particle sizes were 2.6 and 2.1 nm for unpromoted and 6% potassium–promoted catalysts accordingly. This was significantly low as compared to their respective fresh calcined catalysts.

Table 2: Cobalt particle size as estimated by XRD

Catalysts	**Particle Size [nm]**		
	Fresh catalyst (Co_3O_4)	**Reduced catalyst (CoO)**	**Spent catalysts (CoO)**
$15\%Co/Al_2O_3$	9.4	8.8	2.6
$15\%Co\text{-}1\%K/Al_2O_3$	13.2	-	-
$15\%Co\text{-}3\%K/Al_2O_3$	13.4	-	-
$15\%Co\text{-}5\%K/Al_2O_3$	15.6	-	-
$15\%Co\text{-}6\%K/Al_2O_3$	-	13.2	2.1

A direct relationship between cobalt particle size, CO_2 conversion, and product selectivity has been reported. During traditional FT synthesis, methane production usually increases with cobalt particle size decrease and larger particles tend to favor the production of high molecular weight hydrocarbons [27].

3.1.3. Temperature programmed reduction (TPR) analysis

Temperature programmed reduction analyses were performed on $15\%Co/Al_2O_3$ catalysts with different potassium loading to study the catalysts behaviour in the presence of pure H_2; the results are shown in figure 3.

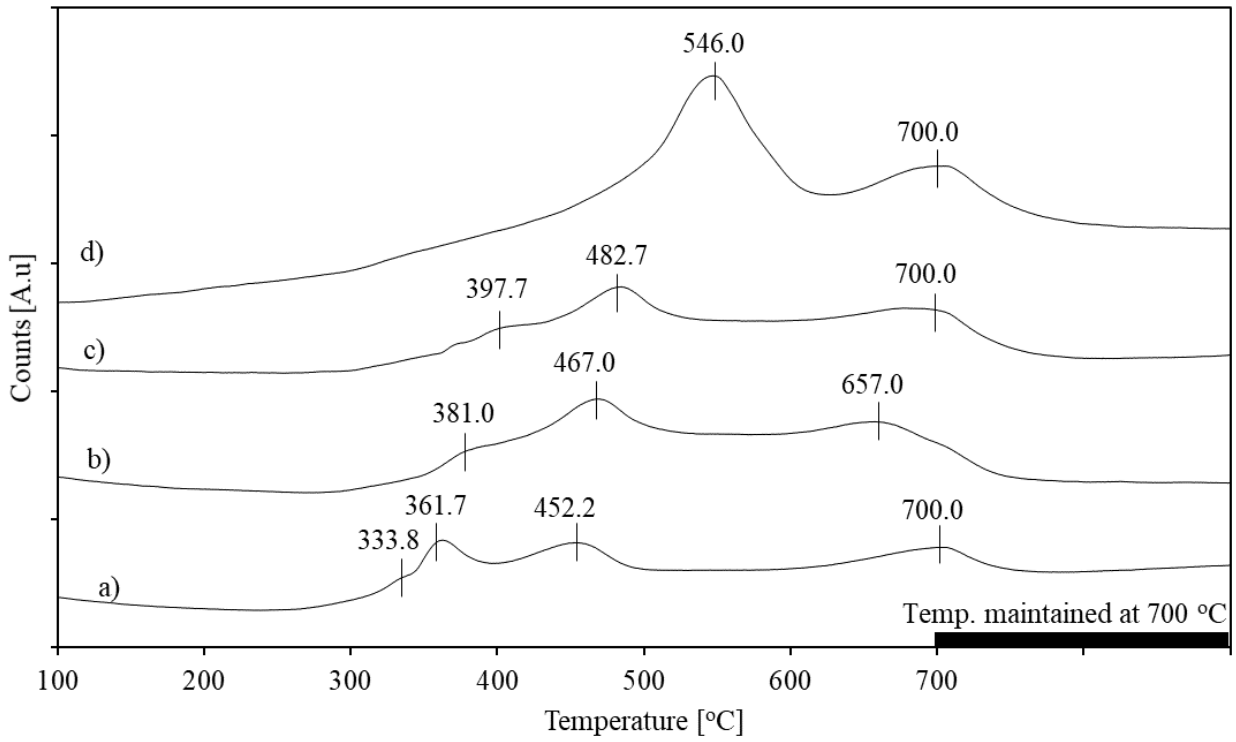

Fig. 3: TPR profiles for a) unpromoted, b) 1% K-promoted, c) 3% K-promoted and d) 5% K-promoted 15%Co/Al_2O_3 catalysts

It can be observed that all the TPR profiles show several overlapping broader reduction peaks, which are associated with several reduction steps. For the unpromoted catalyst, the first reduction peak started at ca. 278.3 ^oC and reached its maximum at 333.8 ^oC when the second peak started to appear, reaching its maximum at ca. 361.7 ^oC. This peak decreased until 400.7 ^oC when the third peak started to appear, reaching its maximum at ca. 452.2 ^oC. This peak decreased until the baseline was established at ca. 501.8 ^oC. The last peak started to appear at ca. 652.5 ^oC, reaching its maximum at 700 ^oC.

The first major peak, which appears at a lower temperature (333.8 ^oC) can be linked to the decomposition of CoN_2O_6. The second and third major peaks, which appear at the temperatures 361.7 and 452.2 ^oC, can be ascribed to the two-step reduction of highly dispersed cobalt oxide species to CoO and Co^0 respectively. The last peak, which appears at a higher temperature (700 ^oC), can be linked to the reduction of cobalt species that strongly interact with the support and are difficult to reduce. These species require more active H_2 for reduction to take place and can only be reduced at elevated temperatures. It was also observed that, as the amount of potassium promoter was increased in the catalysts, the reduction temperature shifted to higher values. For example, comparing the

reduction behaviour of K-free catalyst with 5 wt.% K-promoted catalyst, the reduction temperature increased from 361.7 ^{o}C for K-free catalyst to 546 ^{o}C for 5 wt.% K-promoted catalyst. For unpromoted catalysts, the first two major peaks, which are associated with the two-step reduction of highly dispersed cobalt oxide to CoO and Co^{0} were observed at 361.7 and 452.2 ^{o}C respectively. The last peak representing the reduction of cobalt species, which strongly interacts with the support, was observed at 700 ^{o}C. For 5 wt.% K-promoted catalyst, the peak linked to the two-step reduction was observed at 546 ^{o}C. The last peak associated with the reduction of cobalt species in strong interaction with the support was observed at 700 ^{o}C.

Supported with XPS data, which will be discussed in section 3.1.5, this observation can be linked to metal-support interaction, which has been reported to increase with increasing potassium loading, inhibiting the reducibility of the catalyst to some extent [25].

3.1.4. CO_2-Temperature programmed desorption (CO_2-TPD) analysis

CO_2 – TPD analysis was performed to determine the surface basicity for unpromoted and 6 wt.% K–promoted catalysts. The results are reported in figure 4.

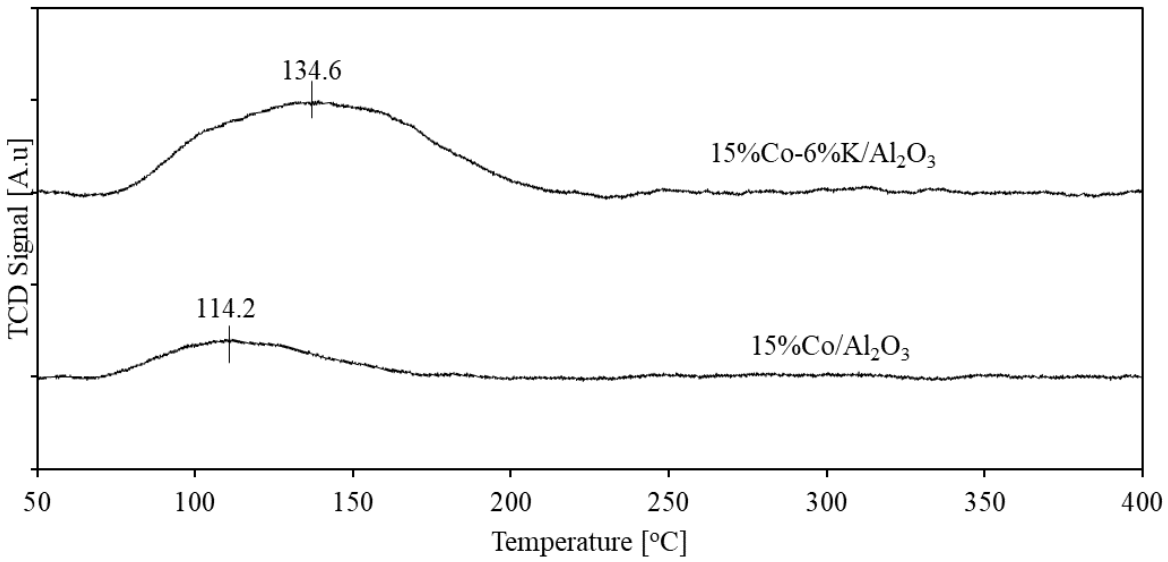

Fig. 4: CO_2 - TPD profiles of reduced catalysts.

A broad peak was present in both TPD profiles at 114.2 ^{o}C and 134.6 ^{o}C for K-free and K-promoted catalysts respectively. For the unpromoted catalyst, the desorption peak started at ca. 71.5 ^{o}C. This peak extended until it reached its maximum at ca. 114.2 ^{o}C, when it started to decrease, reaching the baseline at ca. 171.6 ^{o}C. The K-promoted catalyst displayed a broader desorption peak that extended

to higher temperatures compared to the K-free catalyst. The peak started at ca. 76.7 ^{o}C and extended until it reached its maximum at ca. 134.6 ^{o}C before decreasing until the baseline was established at ca. 210.4 ^{o}C. This indicates that K addition increases the surface basicity of the catalyst, leading to enhanced CO_2 adsorption on the catalyst. These findings agree with Shi *et al.* [19] and Zhang *et al.* [28] who reported that the CO_2 chemisorption was improved while H_2 chemisorption was weakened on the iron-based catalyst surface with the addition of K.

3.1.5. X-ray photoelectron spectroscopy (XPS) analysis

The Co 2p binding energies for the unpromoted and K-promoted catalysts are shown in figure 5.

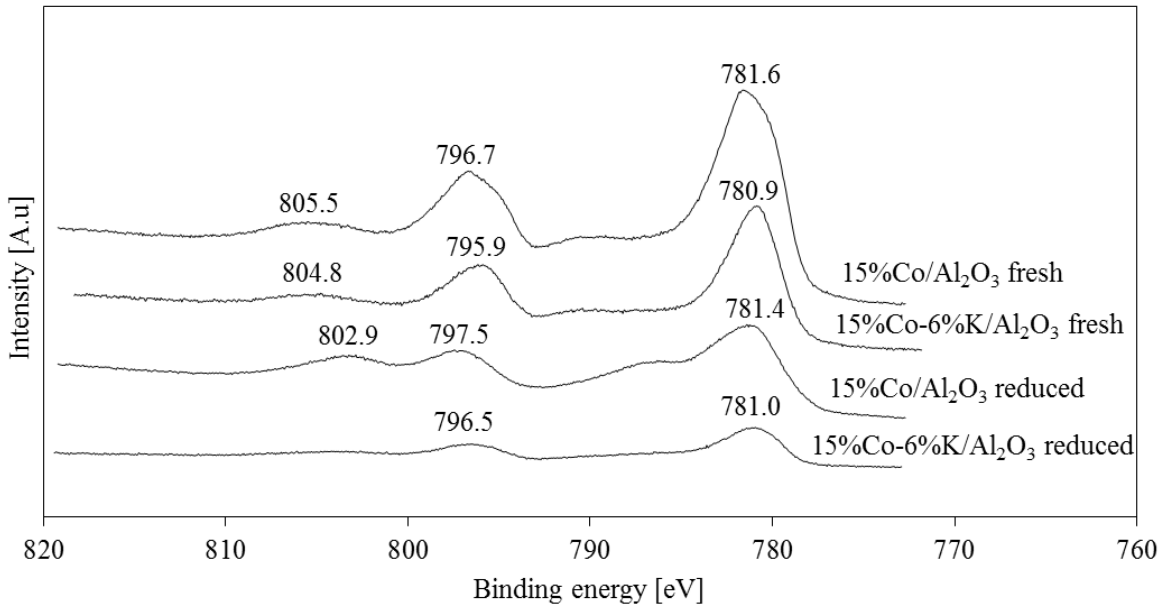

Fig. 5: XPS profiles for unpromoted and K-promoted catalysts.

These data were corrected by setting the binding energy of oxidic O 1s at 531.5 eV [29]. For fresh calcined and unreduced catalyst samples, the binding energies of Co 2p slightly shifted to lower values with the addition of K. As can be seen, for the unpromoted catalyst, the binding energies were 781.6 and 796.7 eV for Co $2P_{3/2}$ and Co $2P_{1/2}$ respectively. They respectively shifted to 780.9 and 795.9 eV when potassium was added. Likewise, for the reduced catalysts, a similar trend was observed. For the unpromoted catalyst, the binding energies of Co 2P decreased with potassium addition, from 781.4 and 797.5 eV to 781.0 and 796.5 eV for Co $2P_{3/2}$ and Co $2P_{1/2}$ respectively. This suggests an electronic modification of cobalt species in the catalyst by K [19].

3.2. Catalyst evaluation

3.2.1 Effect of Temperature

The effect of reaction temperature (195 – 345 ^{o}C) on CO_2 hydrogenation was studied over a 15%Co-5%K/Al_2O_3 catalyst, at 1 bar. It has been reported in the literature that methane is the predominating product during CO_2 hydrogenation using Co/Al_2O_3 catalyst. Promoters such as K [18] have been broadly investigated for Fe-based CO_2 hydrogenation. These promoters are reported to prevent methane generation and promote chain growth probability and boost alkene production. The results are presented in figure 6.

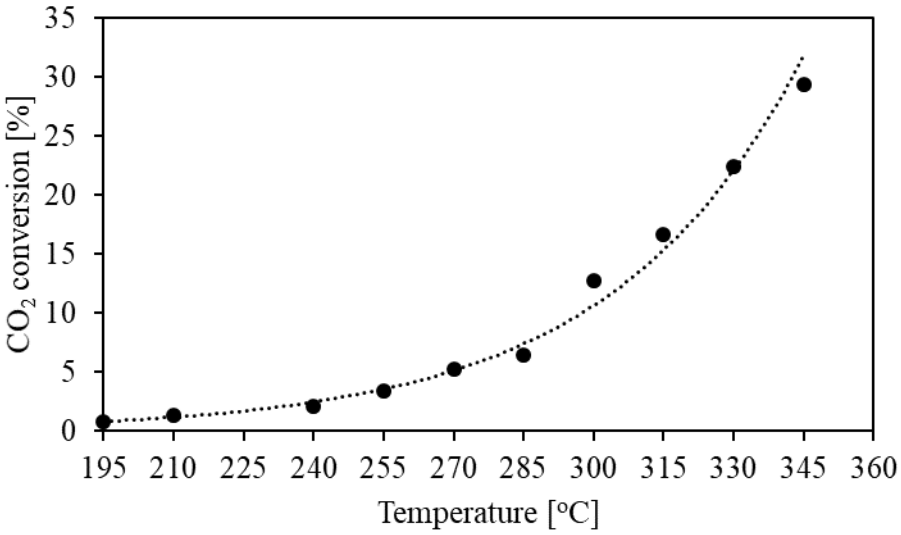

Fig. 6: Effect of reaction temperature on CO_2 conversion.

As the temperature was increased, the CO_2 conversion also increased. At higher temperatures (beyond 285 ^{o}C), this influence was significant. For instance, when the temperature was increased from 285 to 300 ^{o}C, the CO_2 conversion increased from 5.5 to 12.7%. The trend line clearly shows an exponential relationship between the CO_2 conversion and the temperature.

The activation energy of the CO_2 hydrogenation was determined using the Arrhenius plot (fig. 7).

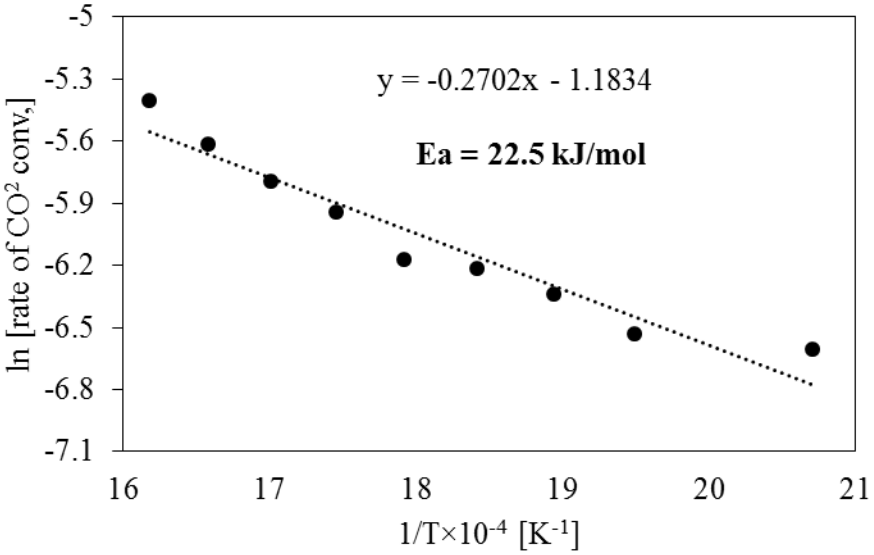

Fig. 7: Arrhenius plot for 15%Co-5%K/Al_2O_3 catalyst

The activation energy for this catalyst was found to be 22.5 kJ/mol. This is significantly lower compared to 77 kJ/mol reported by Mutscler *et al.* [30]. This could be due to a different temperature range of 480 – 510 K and feed gas (H_2:CO_2) ratio of 4:1 used in their study.

Figure 8 shows the effect of temperature on product selectivity.

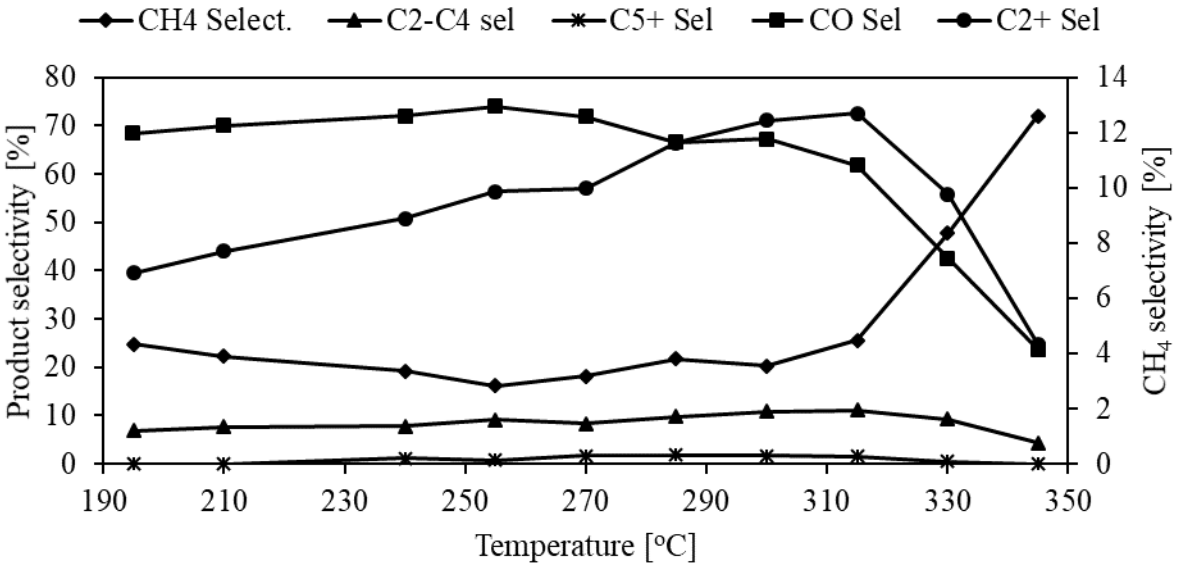

Fig. 8: Effect of reaction temperature on product selectivity (Catalyst: 15%Co-5%K/Al_2O_3; Pressure: atmospheric; space velocity: 1.2 nl/gCat/hr).

As the reaction temperature was increased from 195 to 255 °C, the CO selectivity also increased from 68.3 to 74.0%. Further increase in temperature caused the CO selectivity to decrease, reaching 23.7%

at ca. 345 ^{o}C. In contrast, as the temperature was increased from 195 to 255 ^{o}C, the CH_4 selectivity decreased from 24.8 to 16.1%. Further temperature increase resulted in the CH_4 selectivity increase reaching 71.2% at ca. 345 ^{o}C. On the other hand, the $C_2 – C_4$ selectivity increased from 6.9 to 11.1% when the temperature was increased from 195 to 315 ^{o}C, before decreasing to 4.3% at ca. 345 ^{o}C. Moreover, no C_{5+} hydrocarbons were observed below 240 ^{o}C. The selectivity to C_{5+} hydrocarbons increased from 1.1 to 1.8% as the reaction temperature was increased from 240 to 285 °C before decreasing to 0.5% at ca. 330 ^{o}C. Further increase in the reaction temperature to 345 ^{o}C suppressed the formation of C_{5+}. Nonetheless, the C_{2+} selectivity was observed to increase from 6.9 to 12.7% as the temperature was increased from 195 to 315 ^{o}C, before decreasing to 4.3% at ca. 345 ^{o}C.

Various CO_2 hydrogenation reaction mechanisms have been proposed in the literature. The type of catalyst involved has been reported to play a significant role in the mechanism. On cobalt-based catalysts, it is generally believed that CO_2 hydrogenation proceeds in a two-step reaction mechanism [19]. First, CO_2 is converted to CO as an intermediate product, which is then converted to hydrocarbons through FT synthesis. At higher temperatures, the rate of reaction also increases [31], resulting in the CO formed in the reverse-water-gas-shift reaction (RWGS) being converted to hydrocarbons rapidly; leading to the CO selectivity decreasing and the selectivity of other hydrocarbons improves. At this point, the selectivity of CH_4 increases while the C_2-C_4 and C_{5+} selectivities declined as the temperature increases. The reaction tends to favor CH_4 formation at higher temperatures. It has been reported in earlier studies that according to the Anderson-Schulz-Flory model, the chain growth probability decreases, and methane formation increases at elevated temperatures [32 – 33]. Based on these observations, it can be seen that higher temperatures play a positive role in converting the intermediate CO but at the same time negatively affect the formation of longer chained hydrocarbons while favoring the formation of methane. Therefore, it becomes useful to determine the amount of carbon from CO_2 that does not end up in CH_4. This is achieved by calculating the product yields.

Figure 9 shows the yield of CH_4 and hydrocarbons other than methane (C_{2+}).

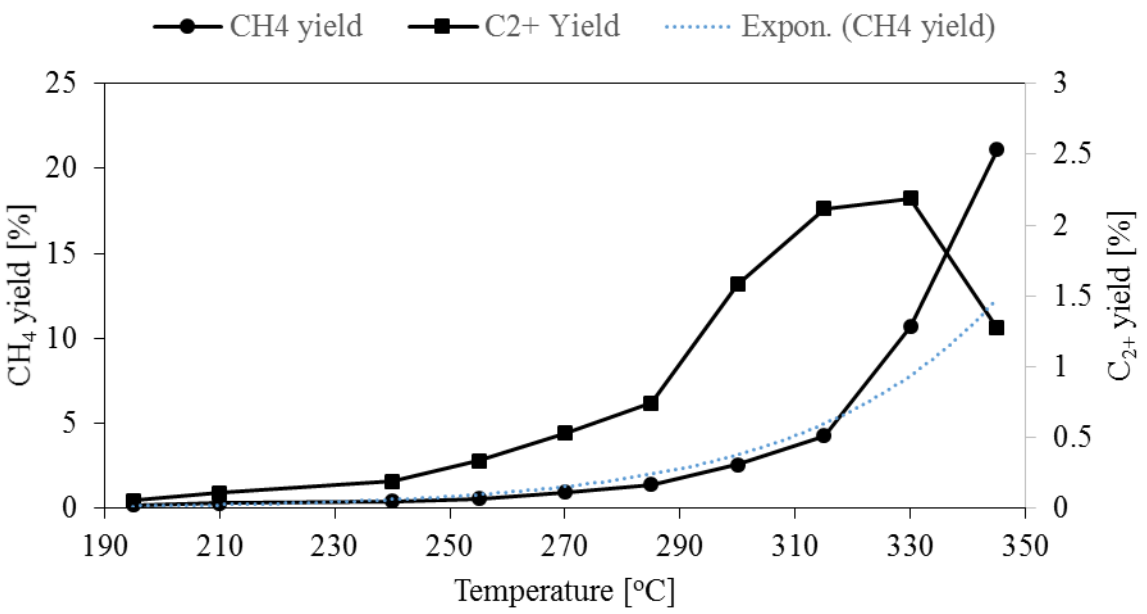

Fig. 9: Effect of reaction temperature on CH_4 and C_{2+} yield during CO_2 hydrogenation.

The methane yield almost exponentially increased with an increase in temperature. For example, as the temperature was increased from 285 to 330 °C, the methane yield increased at a faster rate from 0.88 to ca. 11 %. However, the C_{2+} yield was found to increase with the temperature, reaching its maximum of 2.19% at 330 °C. Further increase in temperature to 345 °C negatively affected the C_{2+} yield as it dropped significantly by almost half to 1.28%.

The increase in C_{2+} yield with the temperature is explained by a concomitant increase in CO_2 conversion (fig. 6) and C_{2+} selectivity (fig. 8) from 190 to 315 °C. Beyond this temperature, the selectivity to C_{2+} products started to decrease, while CO_2 conversion kept increasing. This resulted in a decrease in C_{2+} yield beyond 330 °C. Since the increase in C_{2+} yield with temperature was very low in the range from 190 to 290 °C and that the largest change was recorded when the temperature was increased from 290 to 300 °C, the latter was selected for the rest of the experiments in this study.

3.2.2 Effect of Pressure

The effect of pressure (from 1 bar to 20 bar) was evaluated using 15%Co-5%K/Al_2O_3 catalyst at 300 °C. The data are reported in figure 10.

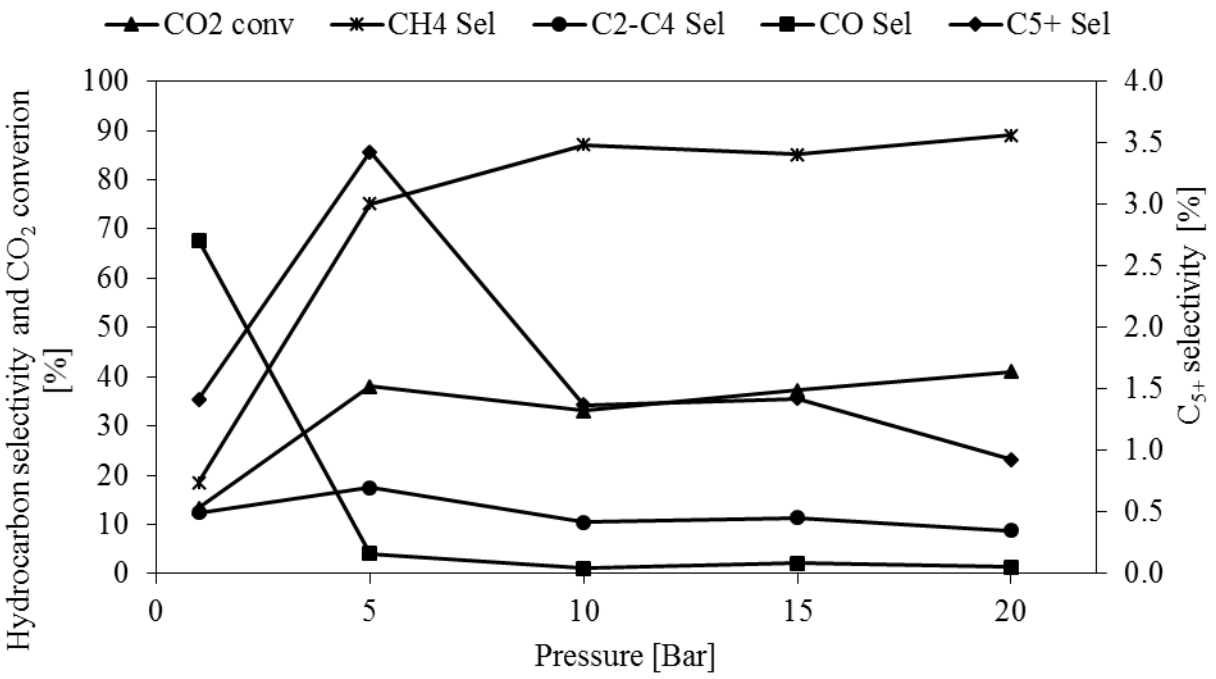

Fig. 10: Effect of reaction pressure on product selectivity and CO_2 conversion.

By increasing the pressure from 1 to 5 bar, the CO_2 conversion significantly increased from 13.3 to 38.0%. This was expected and can be explained by an increase in reactants partial pressures in the reactor. The CH_4, C_2-C_4, and C_{5+} selectivities also increased significantly from 18.5, 12.4, and 1.4 to 75.1, 17.4, and 3.4% respectively. At the same time, the selectivity of CO significantly decreased from 67.7 to 4.0%. As the operating pressure was further increased beyond 5 bar, the CO_2 conversion did not significantly change and was limited at 41.0% at 20 bar. While the CH_4 selectivity continued to increase, reaching its highest value of 88.9% at 20 bar, the CO, C_2-C_4, and C_{5+} selectivities respectively decreased to reach 1.3, 8.8, and 0.93% at 20 bar. The data suggest that higher pressures enhance the methanation ability of the catalyst.

The data in figure 11 shows an increase in CH_4 yield with increasing pressure, while the C_{2+} yield, C_{2+} selectivity, and the chain growth probability, α, increased from 1 bar to 5 bar before decreasing at higher pressures.

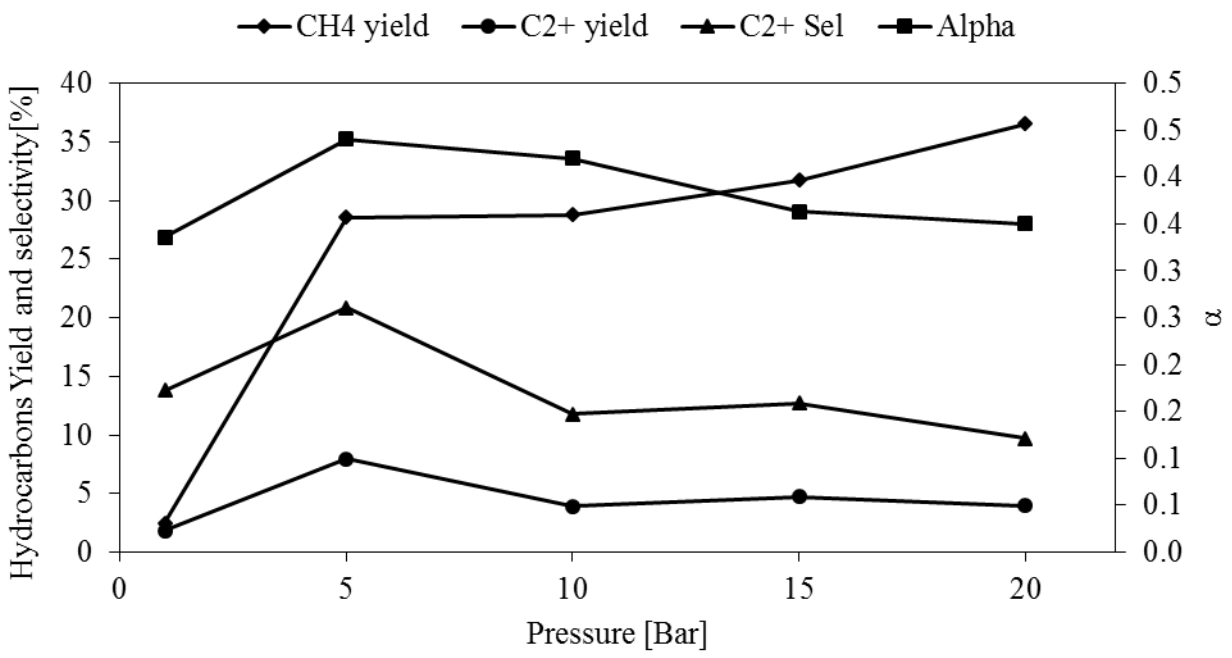

Fig. 11: Effect of pressure on CH_4, C_{2+} yield, C_{2+} selectivity and chain-growth probability (α).

For example, as the pressure was increased from 1 to 5 bar, the CH_4 yield increased from 2.5 to 28.6%. It continued to increase with pressure, up to 36.5% at 20 bar. On the other hand, the C_{2+} yield first increased from 1.83% to 7.9% when the pressure was increased from 1 to 5 bar, before decreasing to values between 3.8 and 4.7% at operating pressures beyond 5 bar. For this reason, 5 bar was selected as the operating pressure for the rest of the experiments in this study.

3.2.3 Effect of potassium loading

Various amounts of potassium were added to the 15%Co/Al_2O_3 catalyst in order to determine the optimal loading of potassium in the catalyst that will maximize the yield of hydrocarbon products other than methane (C_{2+}) during CO_2 hydrogenation. The results obtained are presented in Table 3.

Table 3: Effect of potassium promoter loading on 15%Co/Al_2O_3 catalyst performance during CO_2 hydrogenation (Temperature: 300 ^oC, 5 bar and 1.2 nl/gCat./hr)

Catalyst	**CO_2 conv. (%)**	**CH_4 sel. (%)**	**C_2 - C_4 sel. (%)**	**C_{5+} Sel. (%)**	**CO Sel. (%)**	**CH_4 yield (%)**	**C_{2+} Sel. (%)**	**C_{2+} Yield (%)**	**Alpha***
15%Co/Al_2O_3	33.8	97.0	1.7	0.0	1.3	32.8	1.7	0.6	-
15%Co-1%K/Al_2O_3	34.2	96.4	2.0	0.1	1.6	32.9	2.1	0.7	0.475
15%Co-3%K/Al_2O_3	33.7	91.9	3.2	0.0	4.9	31.0	3.2	1.1	-
15%Co-5%K/Al_2O_3	38.0	75.1	17.4	3.4	4.0	28.6	20.9	7.9	0.440
15%Co-6%K/Al_2O_3	42.3	67.6	22.3	1.9	8.2	28.6	24.2	10.2	0.412
15%Co-8%K/Al_2O_3	12.2	15.9	50.6	0.0	33.5	2.0	50.6	6.2	-

*up to C_6

The product generated was predominantly methane, C_{2+} hydrocarbons and CO. Supported cobalt-based catalysts are commonly used in a traditional FT synthesis with syngas as the feed [34]. Nonetheless, when changing from syngas to CO_2-containing syngas feed (where CO is replaced with CO_2), the reaction tends to shift towards a methanation process. As the potassium promoter content was increased from 0 to 3% on the catalyst, the CO_2 conversion did not change much as it was about 34%. Further increase of potassium content to 5 and 6% resulted in CO_2 conversion increase to 38.0 and 42.3% respectively. The CO_2 conversion then decreased to 12.2% when potassium content was increased to 8%. In contrast, the CH_4 selectivity significantly decreased from 97.0 to 15.9% when potassium content was increased from 0 to 8%. On the other hand, the $C_2 – C_4$ selectivity significantly increased from 1.7 to 50.6% when the potassium loading was increased from 0 to 8%. The C_{5+} selectivity did not show a clear trend, but the highest selectivity was 3.4% at a potassium loading of 5%. The CO selectivity increased from a minimum value of 1.3 to 33.5% when the potassium loading was increased from 0 to 8%. Moreover, the C_{2+} selectivity increased from 1.7 to 50.6% when the potassium loading was increased from 0 to 8%. At the same time, the CH_4 yield significantly decreased from 32.8 to 2.0% when the potassium content was increased from 0 to 8%. Nonetheless, the C_{2+} yield increased from 0.6 to 10.2% when potassium content was increased from 0 to 6%, before decreasing to 6.2% when potassium content was increased to 8%. No clear trend was observed for chain growth probability, α. The chain growth probability was 0.475, 0.440, and 0.412 when potassium content was 1, 5, and 6% respectively.

Based on these observations, we believe that during CO_2 hydrogenation over 15%Co/Al_2O_3 catalysts promoted with different potassium content, CO_2 is first converted to CO through the reverse–water–gas–shift (RWGS) reaction, followed by subsequent hydrogenation of CO to hydrocarbons via modified FT synthesis. In addition, the unpromoted catalyst performed as a methanation catalyst rather than an FT catalyst as the selectivity of CH_4 was found to be 97% when this catalyst was employed [35 – 36]. These results indicate that an appropriate quantity of potassium is required to enhance the catalytic performance for CO_2 hydrogenation to longer chain hydrocarbons. Furthermore, the increase of K loading also improved the selectivity to C_{2+}. As revealed by CO_2-TPD data, the addition of K increased the adsorption of CO_2. During traditional FT synthesis, potassium is known to promote chain growth probability, and the products lean towards heavy molecular weight hydrocarbons [37]. In our case, the chain growth probability did not show a good trend, which makes it difficult to conclude. The optimum potassium loading was found to be 6 wt.% because it produced the highest C_{2+} yield.

4 Conclusions

The main objectives of this study were to evaluate the effect of operating temperature, pressure, and potassium loading on 15%Co/Al_2O_3 Fischer-Tropsch catalyst during CO_2 hydrogenation to liquid hydrocarbons. The reaction temperature and pressure were found to be directly proportional to the CO_2 conversion. At higher temperatures, the rate of reaction increases leading to CO formed in the reverse-water-gas-shift reaction being converted to hydrocarbons faster, as a result, the CO selectivity decrease, and the selectivity of other hydrocarbons improves. The TPR data revealed that potassium loading shifted the catalyst reduction to higher temperatures and increased gradually with the potassium loading increase. This was explained by metal-support interaction, which enhances with increasing potassium loading, and this inhibits the reducibility of the catalyst to some extent. It was also found that potassium improved the surface basicity of the catalyst. XRD exposed that the cobalt particle size increased with potassium loading. A direct relationship between cobalt particle size, CO_2 conversion, and product selectivity exists. Methane formation usually increases with the particle size and larger particles tends to shift products towards longer chain hydrocarbons with very small particles favoring the formation of CO. The optimum potassium loading was 6 wt.%. At higher potassium loading, the methane formation was suppressed and the selectivity of C_{2+} hydrocarbons improved. Based on these observations, it was concluded that for CO_2 hydrogenation to longer chain hydrocarbons over 15%Co/Al_2O_3 catalysts promoted with different potassium loading, CO_2 is first converted to CO via reverse–water–gas–shift reaction, followed by subsequent hydrogenation of CO to hydrocarbons via modified FT synthesis. Nonetheless, the potassium – free catalyst performed as a methanation catalyst rather than an FT catalyst since the selectivity of methane was 97%.

Acknowledgment

Financial support from the National Research Foundation (NRF) and the University of Johannesburg is hereby acknowledged.

References

[1] X.D. Xiaoding, J.A. Moulijn, "Mitigation of CO_2 by chemical conversion: Plausible chemical reactions and promising products", Energy Fuels, 10, (1996) 305–325.

[2] W. Wang, S. Wang, X. Ma, "Recent advances in catalytic hydrogenation of carbon dioxide", Journal of Chemical Society Reviews, 40, (2011) 3703–3727.

[3] K. Stephenne, "Start-up of world's first commercial post-combustion coal fired CCS project: contribution of Shell Cansolv to SaskPower Boundary Dam ICCS project", Energy Procedia, 63, (2014) 6106–6110.

[4] K.M.K. Yu, I. Curcic, J. Gabriel, S.C.E. Tsang, "Recent Advances in CO_2 Capture and Utilization", Chemistry & Sustainability Energy & Materials, 1, (2008) 893–899.

[5] H.A.Zaidi, K.K.Pant, "Catalytic conversion of methanol to gasoline range hydrocarbons", Catalysis Today, 96(3), (2004) 155-160.

[6] P. Kaiser, R.B. Unde, C. Kern, A. Jess, "Production of liquid hydrocarbons with CO_2 as carbon source based on reverse water-gas shift and Fischer-Tropsch synthesis", Chemie Ingenieur Technik, 85, (2013) 489–499.

[7] M.K. Gnanamani, G. Jacobs, W.D. Shafer, D. Sparks, B.H. Davis, "Fischer–Tropsch synthesis: deuterium kinetic isotope study for hydrogenation of carbon oxides over cobalt and iron catalysts", Catalysis Letters, 141, (2011) 1420–1428.

[8] U. Rodemerck, M. Holeňa, E. Wagner, Q. Smejkal, A. Barkschat, M. Baerns, "Catalyst Development for CO_2 Hydrogenation to Fuels", ChemCatChem, 5, (2013) 1948-1955.

[9] J. Wei, J. Sun, Z. Wen, C. Fang, Q. Ge, H. Xu, "New insights into the effect of sodium on Fe_3O_4-based nanocatalysts for CO_2 hydrogenation to light olefins", Catalysis Science & Technology, 6, (2016) 4786-4793.

[10] R. Satthawong, N. Koizumi, C. Song, P. Prasassarakich, "Comparative Study on CO_2 Hydrogenation to Higher Hydrocarbons over Fe-Based Bimetallic Catalysts", Topics in Catalysis, 57, (2014) 588-594.

[11] P. Kangvansura, L.M. Chew, W. Saengsui, P. Santawaja, Y. Poo-arporn, M. Muhler, H. Schulz, A. Worayingyong, "Product distribution of CO_2 hydrogenation by K-and Mn-promoted Fe catalysts supported on N-functionalized carbon nanotubes", Catalysis Today, 275, (2016) 59-65.

[12] M. Albrecht, U. Rodemerck, M. Schneider, M. Bröring, D. Baabe, E.V. Kondratenko, "Unexpectedly efficient CO_2 hydrogenation to higher hydrocarbons over non-doped Fe_2O_3", Applied Catalysis B: Environmental, 204, (2017) 119-126.

[13] B. Zeng, B. Hou, L. Jia, J. Wang, C. Chen, D. Li, Y. Sun, "The intrinsic effects of shell thickness on the Fischer–Tropsch synthesis over core–shell structured catalysts", Catalysis Science & Technology, 3, (2013) 3250-3255.

[14] M.K. Gnanamani, G. Jacobs, R.A. Keogh, W.D. Shafer, D.E. Sparks, S.D. Hopps, G.A. Thomas, B.H. Davis, "Fischer-Tropsch synthesis: Effect of pretreatment conditions of cobalt on activity and selectivity for hydrogenation of carbon dioxide", Applied Catalysis A: General, 499, (2015) 39-46.

[15] R.E. Owen, J.P. O'Byrne, D. Mattia, P. Plucinski, S.I. Pascu, M.D. Jones, "Cobalt catalysts for the conversion of CO_2 to light hydrocarbons at atmospheric pressure", Chemical communications, 49, (2013) 11683-11685.

[16] M.K. Gnanamani, G. Jacobs, H.H. Hamdeh, W.D. Shafer, F. Liu, S.D. Hopps, G.A. Thomas, B.H. Davis, "Hydrogenation of carbon dioxide over Co–Fe bimetallic catalysts", Acs Catalysis, 6, (2016) 913-927.

[17] A.N. Akin, M. Ataman, A.E. Aksoylu, Z.I. Önsan, "CO_2 fixation by hydrogenation over coprecipitated Co/Al_2O_3", Reaction Kinetics and Catalysis Letters, 76, (2002) 265-270.

[18] C.G. Visconti, M. Martinelli, L. Falbo, A. Infantes-Molina, L. Lietti, P. Forzatti, G. Iaquaniello, E. Palo, B. Picutti, F. Brignoli, "CO_2 hydrogenation to lower olefins on a high surface area K-promoted bulk Fe-catalyst", Applied Catalysis B: Environmental, 200, (2017) 530-542.

[19] Z. Shi, H. Yang, P. Gao, X. Li, L. Zhong, H. Wang, H. Liu, W. Wei, Y. Sun, "Direct conversion of CO_2 to long-chain hydrocarbon fuels over K–promoted $CoCu/TiO_2$ catalysts", Catalysis Today, 311, (2018) 65-73.

[20] J. Wei, J. Sun, Z.Y. Wen, C.Y. Fang, Q.J. Ge, H.Y. Xu, "New insights into the effect of sodium on Fe_3O_4-based nanocatalysts for CO_2 hydrogenation to light olefins", Catalysis Science & Technology, 6, (2016) 4786–4793.

[21] J. Zhang, S. Lu, X. Su, S. Fan, Q. Ma, T. Zhao, "Selective formation of light olefins from CO_2 hydrogenation over Fe–Zn–K catalysts", Journal of CO_2 Utilization, 12, (2015) 95–100.

[22] C.G. Visconti, M. Martinelli, L. Falbo, A. Infantes-Molina, L. Lietti, P. Forzatti, G. Iaquaniello, E. Palo, B. Picutti, F. Brignoli, "CO_2 hydrogenation to lower olefins on a high surface area K-promoted bulk Fe-catalyst", Applied Catalysis B: Environmental, 200, (2017) 530–542.

[23] M. Rafati, L. Wang, A. Shahbazi, "Effect of silica and alumina promoters on co-precipitated Fe–Cu–K based catalysts for the enhancement of CO_2 utilization during Fischer–Tropsch synthesis", Journal of CO_2 Utilization, 12, (2015) 34–42.

[24] K. Jalama, "Fischer–Tropsch synthesis over Co/TiO_2 catalyst: Effect of catalyst activation by CO compared to H_2", Catalysis Communications, 74, (2016) 71-74.

[25] M. Khobragade, S. Majhi, K.K. Pant, "Effect of K and CeO_2 promoters on the activity of Co/SiO_2 catalyst for liquid fuel production from syngas", Applied energy, 94, (2012) 385-394.

[26] Y. Zamani, M. Bakavoli, M. Rahimizadeh, A. Mohajeri, S.M. Seyedi, "Synergetic effect of La and Ba promoters on nanostructured iron catalyst in Fischer–Tropsch synthesis", Chinese Journal of Catalysis, 33, (2012) 1119–1124.

[27] J.P. den Breejen, P.B. Radstake, G.L. Bezemer, J.H. Bitter, V. Froseth, A. Holmen, K.P. de Jong, "On the origin of the cobalt particle size effects in Fischer− Tropsch catalysis", Journal of the American Chemical Society, 131, (2009) 7197-7203.

[28] H. Zhang, H. Ma, H. Zhang, W. Ying, D. Fang, "Effects of Zr and K promoters on precipitated iron-based catalysts for Fischer–Tropsch synthesis", Catalysis letters, 142, (2012) 131-137.

[29] M. Jacquemin, M.J. Genet, E.M. Gaigneaux, D.P. Debecker, "Calibration of the X-Ray Photoelectron Spectroscopy Binding Energy Scale for the Characterization of Heterogeneous catalysis: Is everything really under control?", ChemPhysChem, 14 (15), (2013) 3618-3626.

[30] R. Mutschler, E. Moioli, W. Luo, N. Gallandat, A. Züttel, "CO_2 hydrogenation reaction over pristine Fe, Co, Ni, Cu and Al_2O_3 supported Ru: Comparison and determination of the activation energies" Journal of catalysis, 366, (2018) 139-149.

[31] Dry, M.E., "Practical and theoretical aspects of the catalytic Fischer-Tropsch process", Applied Catalysis A: General, 138(2), (1996) 319-344.

[32] M.J. Choi, J.S. Kim, H.K. Kim, S.B. Lee, Y. Kang, K.W. Lee, "Hydrogenation of CO_2 over Fe-K based catalysts in a fixed bed reactors at elevated pressure", Korean Journal of Chemical Engineering, 18(5), (2001) 646-651.

[33] G.P. Van Der Laan, A.A.C.M. Beenackers, "Kinetics and selectivity of the Fischer–Tropsch synthesis: a literature review", Catalysis Reviews, 41(3-4), (1999) 255-318.

[34] R.W. Dorner, D.R. Hardy, F.W. Williams, H.D. Willauer, "Heterogeneous catalytic CO_2 conversion to value-added hydrocarbons", Energy & Environmental Science, 3(7), (2010) 884-890.

[35] R.W. Dorner, D.R. Hardy, F.W. Williams, B.H. Davis, H.D. Willauer, "Influence of Gas Feed Composition and Pressure on the Catalytic Conversion of CO_2 to Hydrocarbons Using a Traditional Cobalt-Based Fischer−Tropsch Catalyst", Energy & Fuels, 23(8), (2009) 4190-4195.

[36] Y. Zhang, G. Jacobs, D.E. Sparks, M.E. Dry, B.H. Davis, "CO and CO_2 hydrogenation study on supported cobalt Fischer–Tropsch synthesis catalysts", Catalysis today, 71(3-4), (2002) 411-418.

[37] J. Gaube, H.F. Klein, “The promoter effect of alkali in Fischer-Tropsch iron and cobalt catalysts”, Applied Catalysis A: General, 350(1), (2008) 126-132.